4-1-2006

# Polystyrene Nanocomposites Based on Quinolinium and Pyridinium Surfactants

Grace Chigwada
*Marquette University*

Dongyan Wang
*Marquette University*

Charles A. Wilkie
*Marquette University*, charles.wilkie@marquette.edu

Accepted version. *Polymer Degradation and Stability,* Vol. 91, No. 4 (April 2006): 848-855. DOI. 

*Polymer Degradation and Stability*, Vol. 91, No. 4 (April 2006): 848-855. DOI. 

# Polystyrene Nanocomposites Based on Quinolinium And Pyridinium Surfactants

Grace Chigqada
Department of Chemistry, Marquette University, Milwaukee, WI
Dongyan Wang
Department of Chemistry, Marquette University, Milwaukee, WI
Charles A. Wilkie
Department of Chemistry, Marquette University, Milwaukee, WI

## Abstract

In this paper pyridine and quinoline-containing salts were employed to modify montmorillonite. TGA analysis shows that the quinolinium modified clay has a higher thermal stability than the pyridinium modified clay. Polystyrene nanocomposites were prepared by in situ bulk polymerisation and direct melt blending using both clays. The X-ray diffraction and transmission electron microscopy results show the formation of intercalated structures. The 50% degradation temperature of the nanocomposites is increased and so is the amount of char from TGA analysis compared to the virgin polymer. Cone calorimetric results indicate that clay reduces the peak heat release rate and average mass loss rate and thus lowers the flammability of the polymer.

## Keywords

Polystyrene, Nanocomposite, Fire retardancy, Surfactants

# 1. Introduction

The study of polymer clay nanocomposites has shown that the insertion of polymer chains into layered silicates dramatically modifies various physical properties, including thermal stability and fire resistance [1], [2]. While a large number of polymer nanocomposite systems have been studied, a great deal of attention has also been focused on polystyrene (PS) clay nanocomposites [3], [4], [5], [6], [7] as studied using cone calorimetry as well as thermogravimetric analysis (TGA). The improvements in physical properties are obtained at very low clay loadings [1], [8], [9], [10].

Natural clays are generally hydrophobic and it is important that they are modified so that the miscibility between the clay and the polymer is enhanced. A cation exchange process achieves the organic modification of the clay; the inorganic cation, usually sodium, is replaced by an organic cation, typically ammonium and phosphonium but other salts such as stibonium [11] and tropylium [12] have also been used. Various ammonium salts have been prepared and in work from this, and other laboratories, it has been shown that the substituents attached to these ammonium salts play a significant role in enhancing the nano-dispersion of the modified clay in the polymer. Clays containing oligomeric units [13], [14] have also been used. The number of alkyl chains attached to the cation has been varied and it is evident that too many alkyl chains results in overcrowding in the gallery space [15], [16], which might result in the formation of an immiscible system. Different substituents have also been investigated and found to have improved thermal stability and offer better dispersion, compared to some commercially available clays.

In this work, ammonium salts containing quinoline and pyridine units have been prepared and these salts were used to modify the clay and polystyrene nanocomposites were prepared by both in situ bulk polymerisation and melt blending processes. This paper shows that the substituents on the ammonium salt and the method used to prepare the nanocomposites play an important role in the dispersion, thermal stability and flammability of both the clay and PS clay nanocomposites.

# 2. Experimental

## 2.1. Materials

The majority of chemicals used in the study, including styrene, polystyrene, diethyl ether, tetrahydrofuran (THF), hexadecyl bromide (C16Br), benzoyl peroxide (BPO), acetone, quinoline and pyridine were obtained from the Aldrich Chemical Company. Montmorillonite was kindly provided by Southern Clay Products, Inc.

## 2.2. Preparation of quinolinium (QC16) salt

The QC16 salt was prepared by the combination of quinoline and hexadecyl bromide (C16Br). In a 250-ml flask was placed 10.0 g (77.4 mmol) quinoline in 150 ml acetone and the solution was stirred for few minutes using a magnetic stirrer. To this solution, 23.6 g (77.4 mmol) hexadecyl bromide (C16Br) was gradually added, and then the mixture was refluxed for 48 h. Most of the solvent was removed under vacuum followed by cooling to RT upon which crystallization occurred. The sample was then filtered and washed with ether. The yield was 5%. $^{1}$H NMR $CDCl_3$: $\delta$ 10.419–10.443 (m, 1H), $\delta$ 9.149 (d, $J$ = 8.4, 1H), $\delta$ 8.358 (d, $J$ = 9.6, 2H), $\delta$ 8.129–8.205 (m, 2H), $\delta$ 7.894–7.947 (m, 1H), $\delta$ 5.364 (t, $J$ = 7.5, 2H), $\delta$ 1.988–2.091 (m, 2H), $\delta$ 1.124–1.252 (m, 26H), $\delta$ 0.807 (t, $J$ = 6.720, 3H).

## 2.3. Preparation of pyridinium (PyC16) salt

PyC16 salt was prepared by a combination of pyridine and hexadecyl bromide (C16Br). In a 250-ml flask was placed 10.0 g (127 mmol) pyridine in 250 ml THF, and the solution was stirred for few minutes using a magnetic stirrer. To this 31.7 g (104 mmol) hexadecyl bromide (C16Br) was gradually added. The mixture was refluxed overnight, followed by cooling to room temperature. A white precipitate was formed which was filtered and washed with ether. The yield was 70%. $^{1}$H NMR $CDCl_3$: $\delta$ 9.449 (d, $J$ = 5.4, 2H), $\delta$ 8.483 (t, $J$ = 7.8, 1H), $\delta$ 8.110 (t, $J$ = 7.2, 2H), $\delta$ 4.983 (t, $J$ = 7.5, 2H), $\delta$ 1.978–2.024 (m, 2H), $\delta$ 1.190–1.294 (m, 26H), $\delta$ 0.838 (t, $J$ = 6.6, 3H).

## 2.4. Organic modification of the clays

A portion of the ammonium salt prepared above was dissolved in 100 ml of THF while the clay was dispersed in 200 ml of 2:1 water:THF; a 20% excess of the ammonium salt, based on the cation exchange capacity, (CEC) of the clay was used. These were mixed and stirred at room temperature for 24 h, followed by filtration and continuous washing with water until no chloride ions were detected using an aqueous silver nitrate solution.

## 2.5. Preparation of polymer clay nanocomposites

Both bulk polymerisation and melt blending processes were utilized for the preparation of PS nanocomposites. The procedures outlined in the literature [17] were used. Briefly, bulk polymerisation involves dispersing the clay and initiator into monomeric styrene, then initiating polymerisation thermally. Melt blending was performed using a Brabender mixer for 15 min at a temperature of about 190 °C at 160 rpm.

## 2.6. Instrumentation

X-ray diffraction (XRD) measurements were performed using a Rigaku powder diffractometer with a Cu tube source ($\lambda$ = 1.54 Å); generator tension was 50 kV at a current of 20 mA. Scans were taken from $2\vartheta$ = 1.0 to 10, step size = 0.1 and scan time per step of 10 s using the high-resolution mode. Bright field transmission electron microscopy (TEM) images of the composites were obtained at 60 kV with a Zeiss 10c electron microscope. The samples were ultramicrotomed with a diamond knife on a Richert-Jung Ultra-Cut E microtome at room temperature to give ~70 nm thick section. The sections were transferred from the knife-edge to 600 hexagonal mesh Cu grids. Thermogravimetric analysis, TGA, was performed on a Cahn TG 131 unit under a flowing nitrogen atmosphere at a scan rate of 20 °C per minute from 20 °C to 600 °C. All TGA experiments have been done in triplicate; the reproducibility of temperature is ±3 °C while the amount of non-volatile residue is reproducible to ±5%. Cone calorimeter measurements at 35 kW $m^{-2}$ were performed using an Atlas Cone 2; the spark was continuous until the sample ignited. All samples were run in triplicate and the average value is reported. Results from cone calorimeter are generally considered to be reproducible to ±10% [18].

# 3. Results and discussion

Two organically-modified clays were prepared using the pyridinium and quinolinium salts, shown in Fig. 1. The thermal stabilities of the organically-modified clays were analysed, and the nanocomposites prepared using these clays were analysed by XRD, TEM, TGA and cone calorimetry.

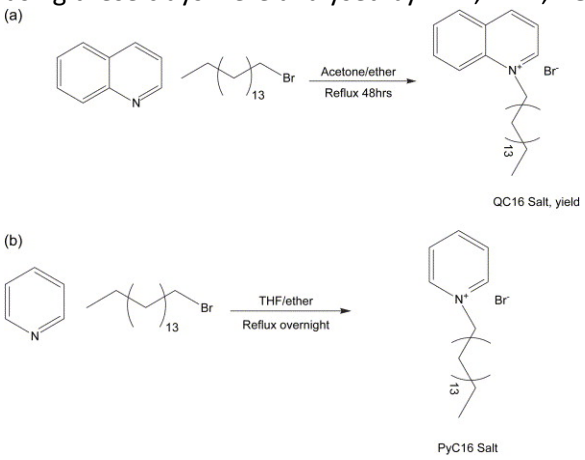


Fig. 1. Preparation of (a) QC16 salt and (b) PyC16 salt.

## 3.1. XRD analysis

Table 1 gives a summary of the d-spacing for both the clays and nanocomposites while Fig. 2, Fig. 3, Fig. 4, Fig. 5 show the XRD curves for the different polymer clay nanocomposites. QC16 modified clay has a d-spacing of 1.8 nm while the nanocomposites prepared using this clay have even greater d-spacing, ranging from 2.9 to 3.4 nm. The increase in the d-spacing suggests the formation of intercalated nanocomposites and hence good compatibility between the modified clay and polystyrene, but the width of the peak suggests that there may be

an immiscible component as well. Generally, it has been shown that for modified clays with a single long chain, an immiscible system is obtained upon melt blending with polystyrene [18]. Here, even though only a single long chain is present, an intercalated system was observed, suggesting that the presence of quinoline as part of the organically-modified clay plays a significant role in enhancing compatibility between the clay and polystyrene.

Table 1. XRD data

| **Sample** | **2ϑ** | **d-Spacing (nm)** |
|---|---|---|
| QC16 clay | 4.8 | 1.8 |
| PyC16 clay | 4.4 | 2.0 |
| PS + 3% QC16 clay, bulk | 2.6 | 3.4 |
| PS + 5% QC16 clay, bulk | 2.6 | 3.4 |
| PS + 3% QC16 clay, MB | 2.8 | 3.2 |
| PS + 5% QC16 clay, MB | 3.0 | 2.9 |
| PS + 3% PyC16 clay, bulk | 3.1 | 2.9 |
| PS + 5% PyC16 clay, bulk | 3.0 | 2.9 |
| PS + 7% PyC16 clay, bulk | 2.9 | 3.0 |
| PS + 3% PyC16 clay, MB | 2.6 | 3.4 |
| PS + 5% PyC16 clay, MB | 2.7 | 3.3 |
| PS + 10% PyC16 clay, MB | 2.7 | 3.3 |

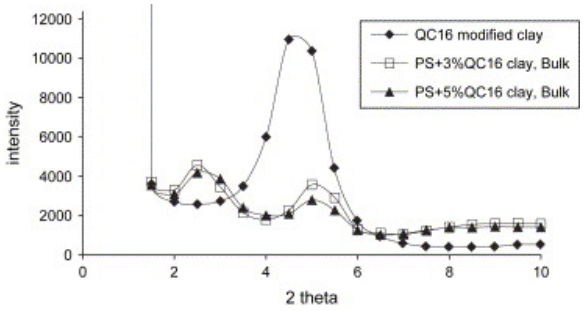

Fig. 2. XRD curves for PS–QC16 clay nanocomposites, bulk.

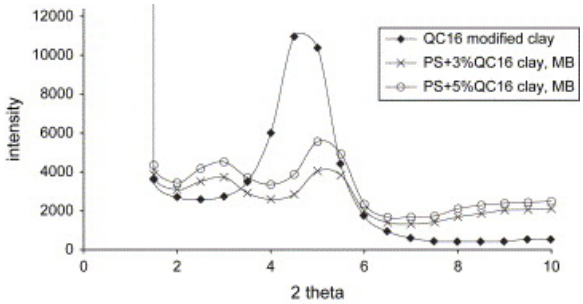

Fig. 3. XRD curves for PS–QC16 clay nanocomposites, MB.

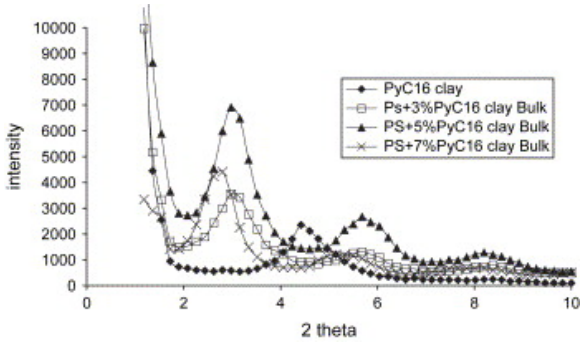

Fig. 4. XRD curves for PS–PyC16 clay nanocomposites, bulk.

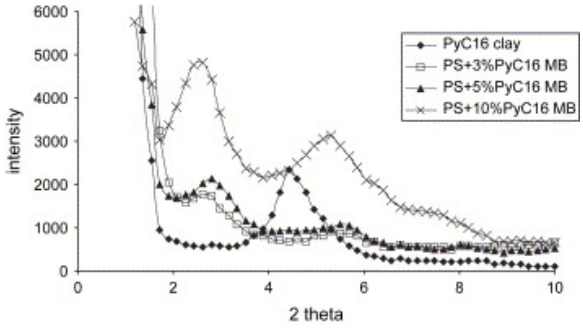

Fig. 5. XRD curves for PS–PyC16 clay nanocomposites, MB.

The same result was observed with nanocomposites prepared using PyC16 modified clay, well-resolved peaks were observed indicating the formation of intercalated nanocomposites as shown in Fig. 4, Fig. 5with d-spacing of about 2.9–3.4 nm. From Table 1, the d-spacing is larger for the melt blended system, but the peaks are sharper for the bulk polymerised sample. These results are consistent with a reasonably good compatibility between the modified clay and polystyrene. This result was further confirmed by transmission electron microscopy.

## 3.2. TEM analysis

Transmission electron microscopy (TEM) was used to characterize the structures of the nanocomposites. Images for samples prepared by both bulk polymerisation and melt blending processes for the two clays are shown in Fig. 6, Fig. 7, Fig. 8, Fig. 9. From the low magnification images, nanocomposites prepared using QC16 modified clay showed tactoids for bulk polymerisation while the samples prepared by melt blending had better dispersion. The high magnification image for the melt blended sample appears to confirm the XRD result of a mixed immiscible/intercalated system, which might explain the broad peaks observed in the XRD.

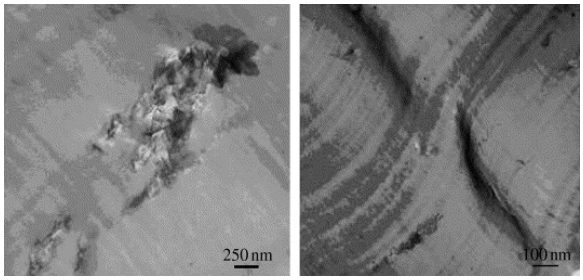

Fig. 6. TEM images for PS–QC16 clay nanocomposites prepared by bulk polymerisation; the low magnification image is on the left and the high magnification image on the right.

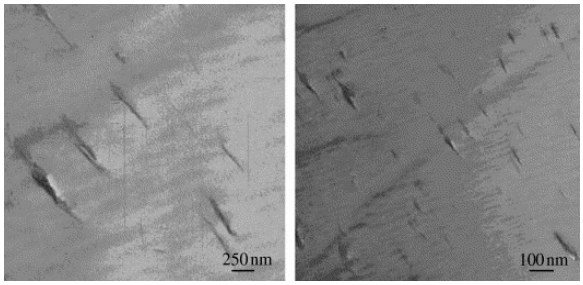

Fig. 7. TEM images for PS–QC16 nanocomposites prepared by melt blending; the low magnification image is on the left and the high magnification image on the right.

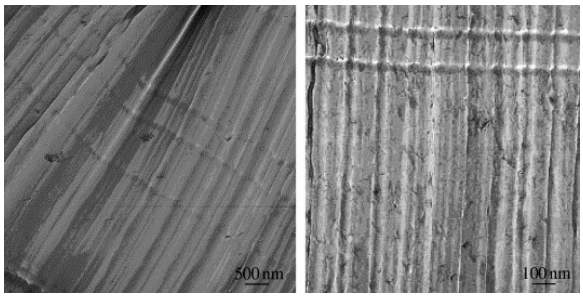

Fig. 8. TEM images for PS–PyC16 nanocomposites prepared by bulk polymerisation; the low magnification image is on the left and the high magnification image on the right.

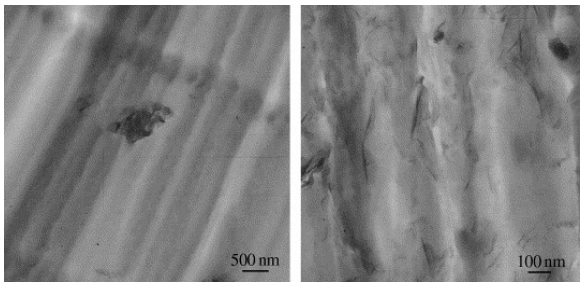

Fig. 9. TEM images for PS–PyC16 nanocomposites prepared by melt blending; the low magnification image is on the left and the high magnification image on the right.

Samples prepared using the PyC16 modified clay show fewer tactoids than the QC16 clay. Surprisingly for this clay, from high magnification images, it seems the melt blended samples have better nano-dispersion than samples prepared by bulk polymerisation. An intercalated system with only a few tactoids was observed, which agrees with the observations from XRD and might mean the position of the positive charge on the cation plays a significant role in the clay dispersion, especially when the data are compared to that of the composites prepared using clay with single long chains by melt blending which results in the formation of microcomposites [18].

## 3.3. Thermogravimetric analysis

One can understand the course of the thermal degradation from thermogravimetric analysis (TGA). The important parameters are the onset temperature of the degradation, which is measured as the temperature at which 10% of the sample is lost, the mid-point of the degradation, another measure of thermal stability and the fraction of material that is non-volatile at 600 °C, known as char [19].

Table 2 and Fig. 10, Fig. 11 show the TGA data and the curves from which the data were extracted. For the two clays, QC16 clay is more thermally stable with an initial degradation temperature of 367 °C and char of about 75% compared to PyC16 clay, which has an initial degradation temperature of 295 °C, and char yield of 70%. This means that QC16 and PyC16 clays have approximately 25% and 30% organic contents, respectively. The difference might be an indication of incomplete exchange during the organic modification, since QC16 cation has a higher molecular weight it should have the larger organic content. Since no peaks were observed at the position where unmodified clay reflections should appear from XRD analysis, the amount of unmodified material must be very negligible. Quinoline is more bulky and might have more difficulty in penetrating the clay gallery than pyridine and this might be why more complete exchange for pyridinium salt was achieved. It is also possible that there is no difference between the yield, since the instrument repeatability is ±3%.

Table 2. TGA analysis data

| **Sample** | $T_{10}$ | $T_{50}$ | **% Char** |
|---|---|---|---|
| PS | 413 ± 2 | 441 ± 2 | 3 ± 3 |
| QC16 modified clay | 367 ± 2 | – | 75 ± 1 |
| PyC16 clay | 295 ± 3 | – | 70 ± 1 |

| | | | |
|---|---|---|---|
| PS + 3% QC16 clay, bulk | 406 ± 3 | 452 ± 2 | 4 ± 2 |
| PS + 5% QC16 clay, bulk | 406 ± 4 | 458 ± 0 | 6 ± 2 |
| PS + 3% QC16 clay, MB | 429 ± 2 | 458 ± 2 | 3 ± 1 |
| PS + 5% QC16 clay, MB | 426 ± 0 | 460 ± 1 | 6 ± 2 |
| PS + 3% PyC16 clay, bulk | 414 ± 0 | 457 ± 1 | 3 ± 3 |
| PS + 5% PyC16 clay, bulk | 409 ± 5 | 459 ± 1 | 6 ± 1 |
| PS + 7% PyC16 clay, bulk | 379 ± 10 | 456 ± 2 | 9 ± 0 |
| PS + 3% PyC16 clay, MB | 422 ± 0 | 455 ± 1 | 4 ± 1 |
| PS + 5% PyC16 clay, MB | 412 ± 1 | 453 ± 1 | 3 ± 1 |
| PS + 10% PyC16 clay, MB | 411 ± 1 | 454 ± 1 | 10 ± 0 |

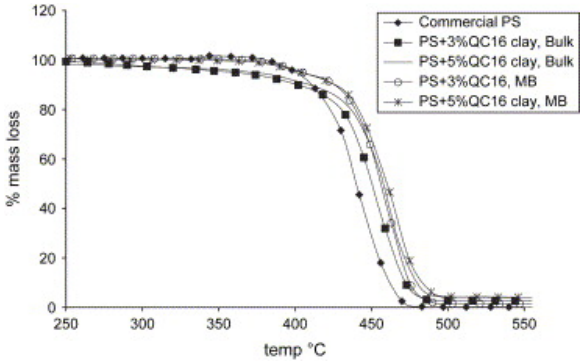

Fig. 10. TGA curves for PS–QC16 clay nanocomposites.

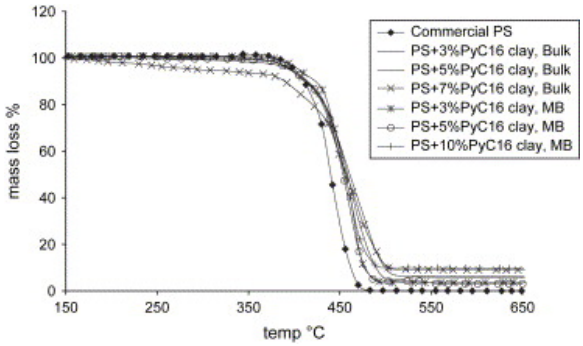

Fig. 11. TGA curves for PS–PyC16 clay nanocomposites.

For the nanocomposites prepared using these clays, a decrease in the initial degradation temperature was observed, while the 50% degradation temperature was improved compared to the virgin polymer. The 50% degradation temperature and the char yield are directly proportional to the clay loading.

## 3.4. Cone calorimetry

Cone calorimetry is used to evaluate the fire properties of polymeric materials. The parameters that may be obtained include the time to ignition ($t_{ign}$), peak heat release rate (PHRR), the time to the peak heat release rate ($t_{PHRR}$), the total heat released (THR), the mass loss rate (MLR) and the specific extinction area (SEA), a measure of smoke. The usual observations for nanocomposites are that the time to ignition is shorter, the PHRR is decreased, the total heat released is unchanged, the mass loss rate is decreased and a somewhat larger amount of smoke is emitted. The decreased time to ignition means that it is actually easier to ignite a nanocomposite than the virgin polymer, which implies higher, rather than lower, flammability. The decrease in PHRR means that the maximum size of the fire is smaller but, since the total heat released is unchanged, everything does eventually burn. The change in the mass loss rate is believed to be the reason for the change in the heat release rate curve. It is impossible to say with certitude what will be required to achieve fire retardancy for nanocomposites but one may make the suggestion that the time to ignition must be increased and the total

heat released must be decreased while maintaining the large reduction in PHRR. The reduction in total heat released means that not all of the sample burns, which implies that either the clay is forming a better barrier or that additives prevent burning.

The flammability parameters evaluated by cone are shown in Table 3 and Fig. 12, Fig. 13, Fig. 14, Fig. 15. From the heat release rate curves it is apparent that for both clays, the peak heat release rate decreases in the presence of clay, with samples prepared by bulk polymerisation giving a better reduction in PHRR than those prepared by melt blending. For both clays, the $t_{ign}$ is shorter for the nanocomposites compared to the virgin polymer. For clays loadings greater than 5% a small reduction in the total heat released is observed for samples prepared by bulk polymerisation. The average mass loss rate was decreased for the nanocomposites compared to the virgin PS.

Table 3. Cone calorimetric data for polystyrene and its nanocomposites

| **Sample** | **$t_{ign}$ (s)** | **PHRR (kW/m$^2$) (% reduction)** | **$t_{PHRR}$, (s)** | **THR (MJ/m$^2$)** | **ASEA (m$^2$/kg)** | **MLR (g/s m$^2$)** |
|---|---|---|---|---|---|---|
| PS | 63 ± 4 | 1351 ± 87 | 126 ± 21 | 100 ± 1 | 1265 ± 23 | 31 ± 1 |
| PS + 3% QC16 clay, bulk | 42 ± 5 | 1100 ± 59 (19) | 131 ± 13 | 95 ± 3 | 1262 ± 23 | 28 ± 1 |
| PS + 5% QC16 clay, bulk | 20 ± 3 | 806 ± 29 (40) | 106 ± 9 | 88 ± 2 | 1317 ± 6 | 22 ± 1 |
| PS + 3% QC16 clay, MB | 63 ± 6 | 998 ± 38 (26) | 139 ± 1 | 94 ± 3 | 1306 ± 30 | 27 ± 0 |
| PS + 5% QC16 clay, MB | 60 ± 2 | 848 ± 29 (37) | 138 ± 6 | 94 ± 3 | 1328 ± 24 | 24 ± 1 |
| PS + 3% PyC16 clay, bulk | 51 ± 4 | 782 ± 70 (42) | 111 ± 10 | 90 ± 3 | 1400 ± 25 | 22 ± 2 |
| PS + 5% PyC16 clay, bulk | 44 ± 4 | 762 ± 8 (44) | 106 ± 2 | 82 ± 2 | 1544 ± 99 | 21 ± 0 |
| PS + 7% PyC16 clay, bulk | 25 ± 4 | 683 ± 28 (50) | 106 ± 6 | 88 ± 4 | 1590 ± 43 | 19 ± 1 |
| PS + 3% PyC16 clay, MB | 58 ± 6 | 1265 ± 55 | 139 ± 16 | 102 ± 6 | 1388 ± 17 | 31 ± 1 |
| PS + 5% PyC16 clay, MB | 49 ± 2 | 1319 ± 77 | 126 ± 7 | 97 ± 3 | 1408 ± 33 | 30 ± 2 |
| PS + 10% PyC16 clay, MB | 47 ± 2 | 1021 ± 28 (24) | 111 ± 8 | 95 ± 4 | 1521 ± 24 | 26 ± 1 |

$t_{ign}$, Time to ignition; PHRR, peak heat release rate; % reduction, [PHRR (polymer) − PHRR (nano)]/PHRR (polymer); $t_{PHRR}$, time to PHRR; THR, total heat released; ASEA, average specific extinction area; MLR, mass loss rate.

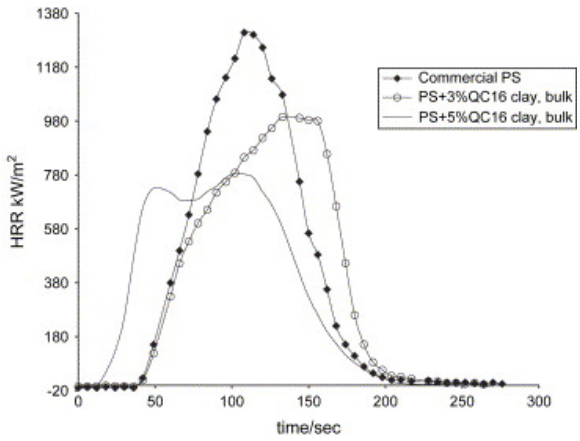


Fig. 12. HRR curves for PS–QC16 clay nanocomposites, bulk.

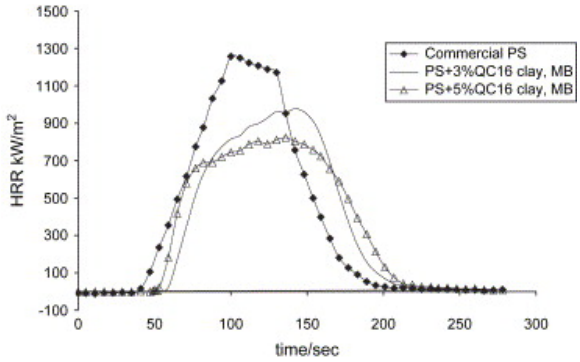

Fig. 13. HRR curves for PS–QC16 clay nanocomposites, melt blending.

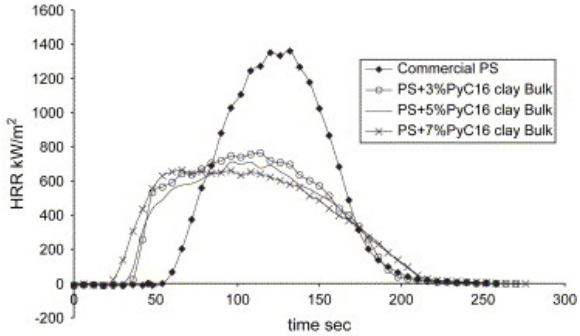

Fig. 14. HRR curves for PS–PyC16 clay nanocomposites, bulk.

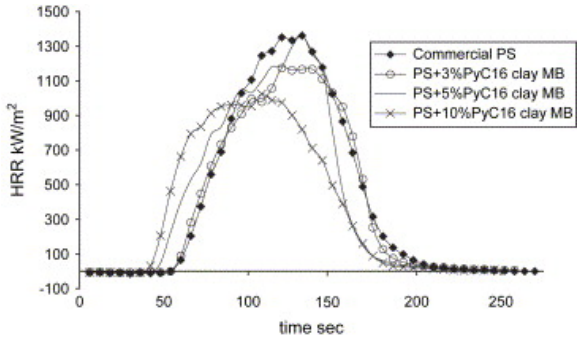

Fig. 15. HRR curves for PS–PyC16 clay nanocomposites by melt blending.

With either of the clays, the PHRR decreases as the clay loading increases especially for samples prepared by bulk polymerisation. For the melt blended samples, nanocomposites prepared using PyC16 clay only show a reduction in PHRR at 10% clay loading while a comparable reduction was obtained at 3% clay loading with QC16 clay. This data correlate well with what was observed from TGA analysis of the clays, which showed that QC16 modified clay is thermally more stable than PyC16 clay.

From XRD, PyC16 clay shows a slightly higher d-spacing, 2.0 nm, than QC16 clay, 1.8 nm. Nanocomposites formed with PyC16 gave a larger d-spacing (3.4 nm) by melt blending compared to 3.0 nm for bulk polymerised samples, while QC16 clay gave a better d-spacing by bulk polymerisation, 3.4 nm, compared to 3.0 nm for melt blending. This might be due to the fact that pyridine is smaller than quinoline so there is more free space in the clay gallery for polymer to penetrate during melt blending for the PyC16 modified clay. By bulk polymerisation, even though QC16 clay is bulky, it is still possible for monomer to penetrate the gallery space due to its smaller size, hence the larger d-spacing. From TGA analysis, QC16 is thermally more stable than PyC16 clay and this may explain why for melt blended samples, QC16 containing nanocomposites have a better reduction in PHRR at the same clay loading compared to PyC16 containing nanocomposites.

## 4. Conclusion

Organic modification of clay results in increased compatibility between the clay and the polymer. Very small changes in the modifier, i.e., replacing pyridine with quinoline results in significant changes in the clay properties. QC16 modified clay showed improved thermal stability compared to PC16 modified clay. For the nanocomposites prepared by melt blending, PyC16 modified clay showed excellent dispersion while QC16 modified clay resulted in good reductions in PHRR at low clay loading. Both clays showed good compatibility with polystyrene and would be effective in nanocomposites formation, however a method that gives good yield of QC16 salt still need to be developed.

## References


[1] M. Alexandre, P. Dubois. *Mater Sci Eng R*, 28 (2000), pp. 1-63

[2] D. Porter, E. Metcalfe, M.J.K. Thomas. *Fire Mater*, 24 (2000), pp. 45-52

[3] R.A. Vaia, H. Ishii, E.P. Giannelis. *Chem Mater*, 5 (1993), pp. 1694-1696

[4] M.W. Noh, C.L. Jackson, A.B. Morgan, P. Harris, S.E. Manias, E.P. Giannelis, *et al.. Chem Mater*, 12 (2000), pp. 1866-1873

[5] J. Zhu, F.M. Uhl, A.B. Morgan, C.A. Wilkie. *Chem Mater*, 13 (2001), pp. 4649-4654

[6] D. Wang, J. Du, J. Zhu, C.A. Wilkie. *Polym Degrad Stab*, 77 (2002), pp. 249-252

[7] M. Okamoto, S. Morita, Y.H. Kim, T. Kotaka, H. Tateyama. *Polymer*, 43 (2000), pp. 1201-1206

[8] Y. Kojima, A. Usuki, M. Kawasumi, A. Okada, Y. Fukushima, T. Kurauchi, *et al. J Mater Res*, 8 (1993), pp. 1185-1189

[9] E.P. Giannelis. *Adv Mater*, 8 (1996), pp. 29-35

[10] T. Lan, P.D. Kaviratna, T.J. Pinnavaia. *Chem Mater*, 6 (1994), pp. 573-575

[11] D. Wang, C.A. Wilkie. *Polym Degrad Stab*, 82 (2003), pp. 309-315

[12] J. Zhang, C.A. Wilkie. *Polym Degrad Stab*, 83 (2004), pp. 301-307

[13] S. Su, D.D. Jiang, C.A. Wilkie. *Polym Degrad Stab*, 83 (2004), pp. 321-331

[14] X. Zheng, C.A. Wilkie. *Polym Degrad Stab*, 82 (2003), pp. 441-450

[15] Chigwada Grace, Jiang David D, Wilkie, Charles A. In: Wilkie CA, Nelson GL, editors. *Fire and polymers: materials and concepts for hazard prevention*, in press.

[16] Chigwada Grace, Jiang David D, Wilkie Charles A. *Thermochim Acta*, in press.

[17] D. Wang, J. Zhu, Q. Yao, C.A. Wilkie. *Chem Mater*, 14 (2002), pp. 3837-3843

[18] J.W. Gilman, T. Kashiwagi, M. Nyden, J.E.T. Brown, C.L. Jackson, S. Lomakin, S. Al-Maliaka, A. Golovoy, C.A. Wilkie (Eds.), *Chemistry and technology of polymer additives*, London Blackwell Scientific (1998), pp. 249-265

[19] A.I. Balabanovich, W. Schnabel, G.F. Levchik, S.V. Levchik, C.A. Wilkie, M. Le Bras, G. Camino, S. Bourbigot, R. Delobel (Eds.), *Fire retardancy of polymeric materials, the use of intumescence,* Royal Society of Chemistry, Cambridge (1998), pp. 236-251